Journal of Medicinal Chemistry

pubs.acs.org/jmc Article

Synthesis and Acidity of 5-(*m*-Terphenyl-2′-yl)-1*H*-tetrazoles: Evidence for an Enhanced Polar–π Effect Compared to Carboxylic Acids

Brett C. Bookser, Quyen-Quyen Do, Yongsak Sritana-Anant, Kim K. Baldridge, and Jay S. Siegel*

Cite This: *J. Med. Chem.* 2021, 64, 3197–3203 Read Online

ACCESS | Metrics & More | Article Recommendations | Supporting Information

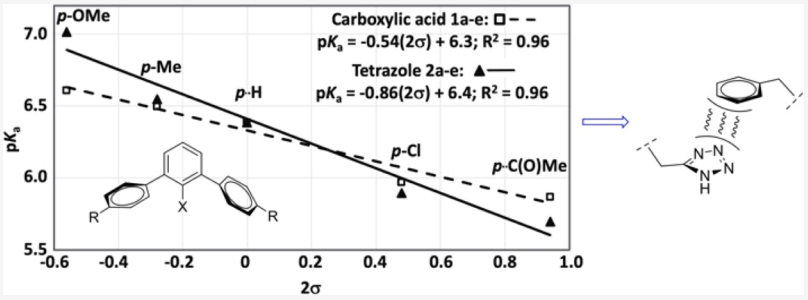

ABSTRACT: The polar–π effect on tetrazoles, medicinal chemistry isosteres of carboxylate, is tested by a Hammett pK_a (microtitration) analysis over a series of 5-(*m*-terphenyl-2′-yl)-1*H*-tetrazoles. A comparison with *m*-terphenyl-2′-yl-carboxylic acids supports the isostere analogy also in response to environmental changes. Computational (B97D/def2TZVPPD) extension of the series plus a scan of solvents (vacuum to water) demonstrates the trend with the dielectric constant. The effect is energetically small but may make statistically significant contributions to the tetrazole pharmacological profile.

INTRODUCTION

Polar–π models[1−3] in (bio)molecular recognition assume that consideration of π-systems as polar groups better accounts for molecular interactions than simply steric bulk and dispersive (VdW) interactions. A typical polar–π functional group would be an aromatic ring because of their general lower reactivity than other π-systems, such as alkenes and carbonyls, and because the first polar moment of benzene is quadrupole polar. The majority of discussions include π–π, cation–π, anion–π, and lone pair–π interactions.[4−8] Hammett series analysis can help establish and quantify through-space polar–π effects as has been studied initially by comparison of pK_a values of 2,6-bis(R-phenyl)benzoic acids **1a**–**e**[9] and later extended for other ionizable groups.[10−14] These terphenyl systems, though not perfectly parallel, allow the study of phenyl-to-X through-space interactions; they model well ligand–protein facial interactions which frequently display similar canted alignments.[4,5]

Tetrazole is considered as a medicinal chemistry isostere for the carboxylic acid functional group and the exchange often results in binding improvements.[15,16] The pK_a values for tetrazoles are similar to comparable carboxylic acids and enzyme binding studies indicate that, in addition to forming salt bridge interactions, their diffuse negative charge gives them an ability to undergo π–π cofacial interactions as an electron-rich aromatic heterocycle.

A survey of the Protein Data Bank (PDB) reveals that cofacial interactions between a tetrazole ligand and a protein aryl residue are common and sometimes occur concomitant with salt bridge binding.[17−19] Additionally, ligated angiotensin II receptor antagonist structures show that tetrazole rings have intramolecular cofacial interactions with ortho-aryl rings that often orient the tetrazole for additional salt bridge binding events.[20−22] Similar polar–π interactions have been invoked when receptor aryl rings stabilize carboxylate salt bridges in a parallel coplanar fashion.[23]

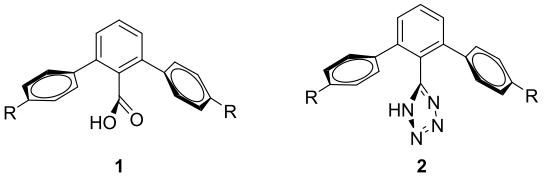

a-h: R = OMe, Me, H, Cl, C(O)Me, NH_2, F, NO_2

Received: December 11, 2020
Published: March 9, 2021

https://dx.doi.org/10.1021/acs.jmedchem.0c02147
J. Med. Chem. 2021, 64, 3197–3203

Scheme 1[a]

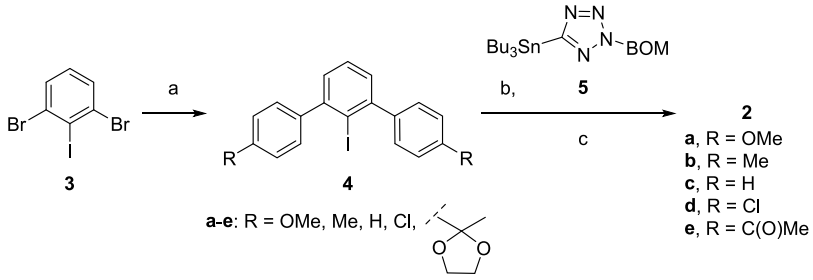

[a]Reagents and conditions: (a) 3 equiv 4-R-PhBr, 3 equiv Mg, cat. I_2, THF, 67 °C/5 h; 6 equiv I_2, 0 °C; (b) 1.2 equiv 5, 0.11 equiv CuI, 0.05 equiv $Pd(PPh_3)_4$ (substitute 0.05 equiv $BnPd(PPh_3)_2Cl$ in preparation of **2d**), toluene, 110 °C/5 h; (c) 8:1 MeOH/6 M HCl, 65 °C/4 h.

The potential character of tetrazole as a polar-aromatic-ring analogue of a carboxylic acid raises the question of how the acidity of the tetrazole group is perturbed by proximal flanking aromatic residues in comparison to the similar effect on the carboxy group. The synthesis of 5-(*m*-terphenyl-2′-yl)-1*H*-tetrazoles **2a−e** and measurement of their pK_a values in methylcellosolve enables a direct head-to-head comparison with the carboxylic acid series **1a−e** (R = OMe, Me, H, Cl, C(O)Me, respectively). Additionally, analogues **1f−h** and **2f−h** (R = NH_2, F and NO_2, respectively) together with **1a−e** and **2a−e** were incorporated into computational studies to explore the widest range of electron-donating and -withdrawing effects on the through-space interaction. The steric interactions between the tetrazole ring and the ortho (flanking) aryl rings should result in a conformation in which the rings are turned out of the plane of the supporting benzene and form a face-to-face arrangement. This arrangement reduces through-bond resonance influence from para-substituents and allows interpretation of substituent effects on pK_a to focus on through-space (polar−π) effects. As in previous studies, the variable Hammett substituents are para- and thus distant to the tetrazole in order to minimize local steric effects.

RESULTS AND DISCUSSION

Chemistry. Synthesis of **2a−e** (Scheme 1) was accomplished by first applying the Hart reaction[24] to **3** to prepare the 2′-iodo-1,1′:3′,1″-terphenyl analogues **4a−e**. Subjecting **4a−e** to Stille cross-coupling with stannane **5**[25] followed by acid hydrolysis completed the tetrazole installation to provide products **2a−e**.

Acidity constant, pK_a, values of tetrazoles **2a−e** were measured in methylcellosolve and compared to the corresponding carboxylates **1a−e** (Table 1). Notably, despite the difference in pK_a values of simple aryl carboxylic acids and tetrazoles,[26] the bis-2,6-(4-R-phenyl) series with R=H display the same values within measurement precision. Consideration of the non-aqueous solvent and steric effects support **1c** and **2c** having similar pK_a values. This coincidence of pK_a values for **1c** and **2c** facilitates an analysis of electron donor and acceptor effects. Both electron-donor-substituted tetrazoles show lesser acidity than the corresponding carboxylic acids; and both electron-acceptor-substituted tetrazoles show greater acidity than the corresponding carboxylic acids. The range of pK_a values (5.7−7.0) corresponds to a change in the energetics of about 2 kcal/mol—highlighting the fact that small changes in energy can shift equilibria substantially.

Table 1. Experimental pK_a Values for Carboxylates 1a−e and Tetrazoles 2a−e[a]

R	σ_n[b]	carboxylate	pK_a[c]	tetrazole	pK_a
OMe	−0.28	**1a**	6.61	**2a**	7.02
Me	−0.14	**1b**	6.50	**2b**	6.55
H	0.00	**1c**	6.39	**2c**	6.39
Cl	0.24	**1d**	5.97	**2d**	5.90
C(O)Me	0.47	**1e**	5.87	**2e**	5.70

[a]Measured by potentiometric titration in methylcellosolve/water (80% w/w), reported values are avg of two runs. [b]See ref 27. [c]See ref 9.

A Hammett analysis plotting of pK_a versus $\Sigma\sigma_{para}$ for tetrazoles **2a−e** (solid line) displays a good linear correlation with a ρ value of −0.86 (Figure 1, solid line). The plot for the corresponding carboxylic acid series **1a−e** (dashed line) is characterized by a ρ of −0.54. This analysis attaches a quantitative character to the relative sensitivity of acidity to substituents for **1** versus **2**. Additionally, the analysis shows that tetrazoles and carboxylic acids are indeed very similar in their response to substitution, with tetrazoles being slightly more sensitive.

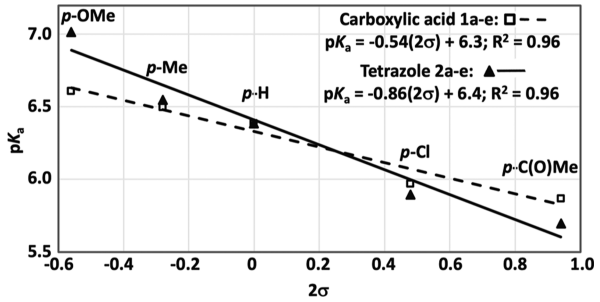

Figure 1. Plot of pK_a values for carboxylates **1a−e** (see ref 9) and tetrazoles **2a−e** versus 2σ values.

Computational Analysis. B97D/Def2-TZVPPD-optimized geometries established a common clinal conformation for the flanking phenyl rings and core acidic functions within the series **1a−h** and **2a−h** and their respective anions **1a−h*** and **2a−h*** (Figure 2), which supports the transfer of substituent effects on the pK_a of the acidic group dominantly by through-space electrostatic and electron dispersion effects from the flanking aryl group's π-face. A reference set in each series (**c**, **f−h**) was chosen to elaborate computational trends across a large range of solvent dielectrics.

Polarity effects vary with changes in the medium, especially the dielectric constant. Computational analysis in six common solvents in addition to the gas phase serve to reveal trends in

https://dx.doi.org/10.1021/acs.jmedchem.0c02147
J. Med. Chem. 2021, 64, 3197−3203

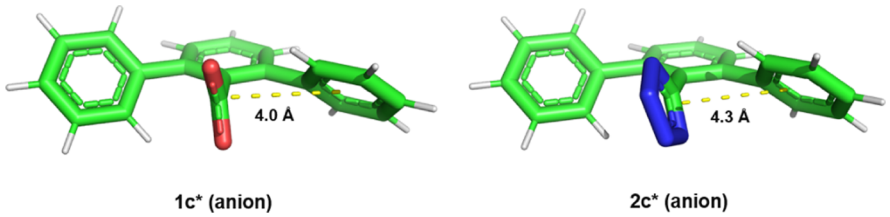

Figure 2. Energy-minimized structures for anions **1c*** and **2c*** in vacuum. For discrete structure files see 1c*-vacuum-b97d_def2tzvppd.pdb and 2c*-vacuum-b97d_def2tzvppd.pdb files in the Supporting Information.

property versus polarity. Relative compound acidity was determined from the computational model reactions: H−CO_2H + X−CO_2H (−) → X−CO_2H + H−CO_2H (−) and H-tetrazole + X-tetrazole (−) → X-tetrazole + H-tetrazole (−) [see the Experimental Section for details]. Changes in compound acidity (ΔpK_a values) were analyzed with respect to the dielectric constant of the medium (gas = 0, benzene = 2.27, THF = 7.43, acetone = 20.49, acetonitrile = 36.64, DMSO = 46.83, water = 78.36) and with respect to Hammett σ_{para} values of the substituents (NH_2 = −0.66; F = +0.06; NO_2 = +0.78).

Computations predict a monotonic trend of increasing pK_a values along the series **1f−h** as well as **2f−h** (Figures 3 and 4).

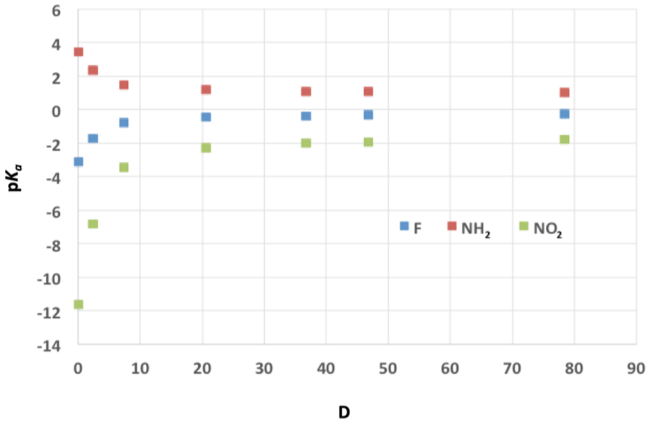

Figure 3. B97D/Def2-TZVPPD pK_a trends of carboxylic acids **1f−h** in solvents of dielectric 0−78 using the model reaction H−CO_2H + X−CO_2H (−) → X−CO_2H + H−CO_2H (−).

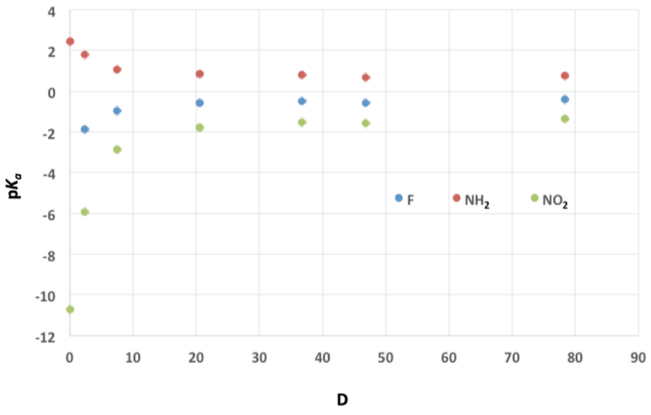

Figure 4. B97D/Def2-TZVPPD pK_a trends of 1*H*-tetrazoles **2f−h** in solvents of dielectric 0−78 using the model reaction H-tetrazole + X-tetrazole (−) → X-tetrazole + H-tetrazole (−).

The order in the series is maintained across dielectric values from vacuum to water. The dynamic range in ΔpK_a for series **1** begins at 15.7 in vacuum and reduces asymptotically to 2.8 in water; for series **2**, the values are 13.1 and 2.1, respectively. The pronounced differentiation in vacuum diminishes rapidly with increasing dielectric constant, and from 20 to 80 D the change is very gradual. The difference between the behavior in vacuum versus water is halved in benzene (2.2 D) and reduced by over 90% in acetone (20.2 D). This behavior is consistent with long established models for polarity.

Hammett ρ slopes quantify the sensitivity of compound acidity to substituent effects; they can vary in different solvents. Acidity in methylcellosolve/water is not easily calculated by continuum solvent models, but the trend of ΔpK_a as a function of solvent allows interpolation of the approximate expected values (*cf* Figures 3 and 4). As such, we can see that the slope predicted from the B97D/Def2-TZVPPD level calculations for series **2** agrees well with that found experimentally; however, for series **1** the computational value is higher. Therefore, the computational model predicts carboxylate to be more sensitive than tetrazole, which is the reverse of what was measured for series **1** and **2** but is consistent with solvent polarity trends for simple carboxylate (e.g., benzoic acid) versus tetrazole acidity. Specific-solvent-molecule models can influence detailed quantitative carboxylic acid predictions but are outside the scope of this study.[28] Overall, the energy differences necessary to flip the trends are small (<1 kcal/mol), so care must be taken in interpretation.

The observation that 5-(phenyl)tetrazole is more acidic[26] than tetrazole **2c** in comparable media could in principle stem from through-bond (resonance and inductive) or through-space (bulk steric, general dielectric, specific electrostatic) effects. The inductive effect of phenyl substitution would predict **2c** to be more acidic and the twist out of plane minimizes any resonance effects. In addition, *p*-X-benzoic acids and 5-(*p*-X-phenyl)-1*H*-tetrazoles display similar ρ slopes (see the Supporting Information)[26] but of lower magnitude than for the series **2** for a shorter bond path; therefore, through-bond effects cannot be the dominant influence. Assuming that the 2,6-*p*-R-diaryl groups maintain a constant steric effect across the series, the trend origin should lie with either general dielectric or specific electrostatic patterning. The sensitivity of reported tetrazoles and benzoic acids to the solvent shows that this cannot be a simple effect due to the dielectric of the medium,[29−31] which highlights an electrostatic patterning ala Hunter−Sanders as a working model for the variation.[2,32] The tetrazole ring in series **2** has greater contact surface with the flanking arenes and less direct solvent contact compared to COOH in the cognate series studied previously.

Analysis of the PDB X-ray structure database reveals several examples of tetrazole cofacial interactions with protein aryl groups (see PDB structures 1A8T,[17] 4L34,[18] 5YVA,[19]

https://dx.doi.org/10.1021/acs.jmedchem.0c02147
J. Med. Chem. 2021, 64, 3197−3203

4ZUD,[21] and the Supporting Information for images), which highlights specific aryl-tetrazole through-space interactions of medicinal chemistry relevance. This study highlights that the relative acidity of tetrazole and carboxylic acid bearing small molecule drugs can depend on the nature of the medium as well as specific electrostatic patterns in the binding pocket. When translated to an ADME, PK/PD, or binding profile, this could translate into differences in membrane permeability, susceptibility to oxidation, or protonation state as the molecule navigates its voyage from absorption to excretion. Increased polarizability for the tetrazole favors its interaction with aromatic side chains, assuming a similar state of protonation and therefore having a quantitative face on the isosteric relationship of tetrazole and carboxylate could inform drug design on the reasonable limits of such effects.

CONCLUSIONS

Investigation of the acidity of a Hammett series of substituted 2,6-bis(R-phenyl)phenyltetrazoles shows a linear relationship and slope similar to the isosteric carboxylic acids. In addition to being an isostere of the carboxylic acid, tetrazole can also be viewed as an aromatic heterocycle. Specific noteworthy points derived from this study include the following: (1) tetrazole **2c** and carboxylic acid **1c** have almost identical pK_a values which would not be the case for simple dielectric effects; (2) tetrazole is sensitive to through-space interactions with the flanking aryl rings that are essentially repulsive to the ionized (anionic) state; and (3) the details of the interaction lie with the intimate structure of the contact surface and its electron density.

Polar−π effects enter the analysis in two ways: the tetrazole ring−arene interaction and the tetrazole anion−arene interaction. This study shows that tetrazole rings may have an enhanced interaction with cofacial aryl rings compared to carboxylic acids but that in any case the energetics of variation are small and in the range of lead fine optimization, where small changes in the energy landscape importantly affect the pharmaceutical profile of a drug molecule.

Despite polar−π effects being invoked broadly in the literature of biorecognition events,[4,5] the complexity of these systems obfuscates the degree to which energy factorization is warranted. Model studies such as that presented here isolate and highlight specific interactions. Quantum chemical computations refine the physical model. In combination, these studies reveal how even small energy differences manifest clear influences on molecular properties; however, they also point to the environmental dependence of these effects such that caution is warranted when transferring between simplified *in vitro* models and complex *in vivo* pharmacology. Caveats recognized, when protein−ligand structural analysis reveals aromatic-ring propinquity in a ligand−protein complex, judicious consideration of polar−π aspects should assist the discovery of molecular designs with improved overall drug product pharmaceutical profile.

EXPERIMENTAL SECTION

General Procedures. Commercial chemicals were used as supplied unless otherwise stated. Dry tetrahydrofuran was obtained by distillation over sodium and benzophenone. Thin-layer chromatography (TLC) was performed on aluminum-backed silica gel 60 F_{254} plates from Altech. Flash chromatography (FC) was performed with silica gel (230−425 mesh) from Fisher Scientific Company. Melting point determinations were performed on a Mel-Temp apparatus to ±1 °C precision. ^{1}H and ^{13}C NMR spectra were recorded on Varian 400 MHz and 500 MHz/Unity spectrometers, respectively. Chemical shifts are reported in ppm. ^{1}H NMR was reported as δ relative to tetramethylsilane at 0.00 ppm. ^{13}C NMR spectra were referenced to 76.9 ppm in $CDCl_3$ and 39.7 ppm in DMSO-d_6. High-resolution mass spectrometry (HRMS) analysis was obtained using positive ionization mode with a TOF mass analyzer, which provided values for samples **2a−2e** with errors of <0.003 m/z from calculated values and this was used to assign purities >95%. These data were obtained from the University of California at Riverside mass spectrometry facility.

General Method A. Synthesis of 2′-iodo-1,1′:3′,1″-terphenyl analogues **4a−e.** To magnesium turnings (1.17 g, 48.2 mmol, 3 equiv), I_2 (5 mg) and 5 mL THF at 67 °C was added in a dropwise manner the 4-substituted-bromobenzene (48.2 mmol, 3 equiv) as a solution in 50 mL of THF and the mixture stirred at 67 °C for 5 h. This solution was cooled to 0 °C, and a solution of 2,6-dibromoiodobenzene (**3**) (5.81 g, 16 mmol, 1 equiv) in 60 mL of THF was added in a dropwise manner. The resulting solution was stirred at rt for 5 h. Then, the solution was cooled to 0 °C and I_2 (7.11 g, 28 mmol, 1.75 equiv) was added. The resulting mixture was stirred at rt for 1 h. Then, the mixture was washed with aqueous 10% $Na_2S_2O_3$, water, and brine, dried ($MgSO_4$), and rotary-evaporated. Purification by FC (SiO_2, hexane to CH_2Cl_2 gradient) provided the title products **4a−e**.

*2′-Iodo-4,4″-dimethoxy-1,1′:3′,1″-terphenyl (**4a**).* General method A was followed, starting with 4-bromoanisole as the 4-substituted-bromobenzene for Grignard formation. White solid; yield 29%; mp 136 °C. ^{1}H NMR (500 MHz, $CDCl_3$): δ 7.32 (1H, t, J = 8 Hz), 7.28 (4H, d, J = 9 Hz), 7.20 (2H, d, J = 8 Hz), 6.94 (4H, d, J = 9 Hz), 3.82 (6H, s); ^{13}C NMR (125 MHz, $CDCl_3$): δ 159.0, 147.7, 138.3, 130.5, 128.6, 127.5, 113.2, 105.0, 55.1. HRMS (EI+): m/z calcd for $C_{20}H_{17}IO_2$ [M+]: 416.0273; found, 416.0291.

*2′-Iodo-4,4″-dimethyl-1,1′:3′,1″-terphenyl (**4b**).* General method A was followed, starting with 4-bromotoluene as the 4-substituted-bromobenzene for Grignard formation. White solid; yield 25%; mp 135−136 °C (lit.[33] mp 120 °C). ^{1}H NMR (500 MHz, $CDCl_3$): δ 7.37 (1H, t, J = 7 Hz), 7.22−7.28 (10H), 2.41(6H, s); ^{13}C NMR (125 MHz, $CDCl_3$): δ 148.1, 143.0, 137.3, 129.4, 128.6, 128.6, 127.6, 104.2, 21.2. HRMS (EI+): m/z calcd for $C_{20}H_{17}I$ [M+]: 384.0375; found, 384.0373.

*2′-Iodo-1,1′:3′,1″-terphenyl (**4c**).* General method A was followed, starting with bromobenzene as the 4-substituted-bromobenzene for Grignard formation. White solid; yield 25%; mp 110 °C (lit.[24] mp 113.5−115 °C). ^{1}H NMR (500 MHz, $CDCl_3$): δ 7.36−7.45(11H, m), 7.26 (2H, d, J = 8 Hz); ^{13}C NMR (125 MHz, $CDCl_3$): δ 148.2, 145.7, 129.5, 128.7, 127.9, 127.6, 127.6, 103.7. HRMS (EI+): m/z calcd for $C_{18}H_{13}I$ [M+]: 356.0062; found, 356.0076.

*4,4″-Dichloro-2′-iodo-1,1′:3′,1″-terphenyl (**4d**).* General method A was followed, starting with 1-bromo-4-chlorobenzene as the 4-substituted-bromobenzene for Grignard formation. White solid; yield 84%; mp 127 °C. ^{1}H NMR (500 MHz, $CDCl_3$): δ 7.42 (4H, d, J = 8 Hz), 7.40 (1H, t, J = 8 Hz), 7.30 (4H, d, J = 8 Hz), 7.24 (2H, d, J = 8 Hz); ^{13}C NMR (125 MHz, $CDCl_3$): δ 147.1, 143.8, 133.8, 130.8, 128.9, 128.3, 127.9, 103.4. HRMS (EI+): m/z calcd for $C_{18}H_{11}Cl_2I$ [M+]: 423.9283; found, 423.9286.

*2,2′-(2′-Iodo-[1,1′:3′,1″-terphenyl]-4,4″-diyl)bis(2-methyl-1,3-dioxolane) (**4e**).* General method A was followed, starting with 2-(4-bromophenyl)-2-methyl-1,3-dioxolane as the 4-substituted-bromobenzene for Grignard formation. White solid; yield 66%; mp 141 °C. ^{1}H NMR (500 MHz, $CDCl_3$): δ 7.47 (4H, d, J = 8 HZ), 7.29 (1H, t, J = 8 Hz), 7.26 (4H, d, J = 8 Hz), 7.15 (2H, d, J = 8 Hz), 3.98 (4H), 3.77 (4H), 1.63 (6H, s); ^{13}C NMR (125 MHz, $CDCl_3$): δ 147.9, 145.0, 142.5, 129.3, 128.7, 127.6, 124.8, 108.8, 103.3, 64.5, 27.4. HRMS (EI+): m/z calcd for $C_{26}H_{25}IO_4$ [M+]: 528.0798; found, 528.0780.

General Method B. Synthesis of 5-([1,1′:3′,1″-terphenyl]-2′-yl)-1H-tetrazoles **2a−e**. A mixture of 2′-iodo-1,1′:3′,1″-terphenyl analogue **4** (0.65 mmol, 1 equiv), [2-(benzyloxymethyl)-5-(tributylstannyl)-2*H*-tetrazole[25] (0.77 mmol, 1.2 equiv), copper(I) iodide (0.071, 0.11 equiv), tetrakis(triphenylphosphine)palladium(0) (0.03

https://dx.doi.org/10.1021/acs.jmedchem.0c02147
J. Med. Chem. 2021, 64, 3197−3203

mmol, 0.05 equiv), and 8 mL of toluene was heated at 110 °C for 5 h. Then, the mixture was cooled to rt and filtered through Celite and solvent rotary-evaporated. The residue was purified by FC (SiO_2, hexane to EtOAc gradient) to provide the intermediate product. This intermediate, 5 mL of methanol and 0.63 mL of 6 M HCl were stirred at 65 °C for 4 h; then, the solvent was removed by rotary evaporation. The residue was dissolved into 1 M NaOH and extracted with EtOAc (2×). The separated aqueous layer was treated with a minimal amount of 6 M HCl, which resulted in the formation of a solid suspension. The mixture was extracted with EtOAc (3×). Then, the organic extract was dried ($MgSO_4$) and evaporated to provide the title product **2**.

*5-(4,4″-Dimethoxy-[1,1′:3′,1″-terphenyl]-2′-yl)-1H-tetrazole (**2a**).* General method B was followed. White solid; yield 65%; mp 228−230 °C. ^{1}H NMR (500 MHz, DMSO-d_6): δ 7.70 (1H, t, J = 9 Hz), 7.46, (2H, d, J = 9 Hz), 6.99 (4H, d, J = 9 Hz), 6.81 (4H, d, J = 9 Hz), 3.70 (6H, s); ^{13}C NMR (125 MHz, DMSO-d_6): δ 158.6, 153.7, 142.7, 131.9, 130.7, 129.9, 123.0, 113.6, 55.0. HRMS (EI+): m/z calcd for $C_{21}H_{18}N_4O_2$ [M − H+]: 357.1352; found, 357.1355.

*5-(4,4″-Dimethyl-[1,1′:3′,1″-terphenyl]-2′-yl)-1H-tetrazole (**2b**).* General method B was followed. White solid; yield 51%; mp 243−244 °C. ^{1}H NMR (500 MHz, DMSO-d_6): δ 7.73 (1H, t, J = 8 Hz), 7.50, (2H, d, J = 8 Hz), 7.06 (4H, d, J = 8 Hz), 6.81 (4H, d, J = 8 Hz), 2.24 (6H, s); ^{13}C NMR (125 MHz, DMSO-d_6): δ 152.6, 142.9, 136.7, 136.4, 130.8, 129.0, 128.7, 128.5, 122.1, 20.4.

*5-([1,1′:3′,1″-Terphenyl]-2′-yl)-1H-tetrazole (**2c**).* General method B was followed. White solid; yield 87%; mp 242−248 °C. ^{1}H NMR (400 MHz, DMSO-d_6): δ 7.75(1H, t, J = 8 Hz), 7.53 (2H, d, J = 8 Hz), 7.24 (6H, m), 7.07 (4H, t, J = 4 Hz); ^{13}C NMR (125 MHz, DMSO-d_6): δ 153.2, 143.1, 139.5, 131.1, 129.4, 128.7, 128.2, 127.5, 122.5. HRMS (EI+): m/z calculated for $C_{19}H_{14}N_4$ [M − H+]: 297.1140; found, 297.1151.

*5-(4,4″-Dichloro-[1,1′:3′,1″-terphenyl]-2′-yl)-1H-tetrazole (**2d**).* General method B was followed except that *trans*-benzyl(chloro)bis-(triphenylphosphine)palladium(II) (0.05 equiv) was substituted for tetrakis(triphenylphosphine)palladium(0). White solid; yield 51%; mp 228−230 °C, dec. ^{1}H NMR (500 MHz, DMSO-d_6): δ 7.78 (1H, t, J = 8 Hz), 7.58, (2H, d, J = 8 Hz), 7.34 (4H, d, J = 9 Hz), 7.08 (4H, d, J = 9 Hz), 3.70 (6H, s); ^{13}C NMR (125 MHz, DMSO-d_6): δ 153.3, 141.8, 138.2, 132.6, 131.2, 130.6, 129.7, 128.3, 122.7; HRMS (EI+): m/z calcd for $C_{19}H_{12}Cl_2N_4$ [M − H+]: 365.0361; found, 365.0371.

*1,1′-(2′-(1H-Tetrazol-5-yl)-[1,1′:3′,1″-terphenyl]-4,4″-diyl)bis-(ethan-1-one) (**2e**).* General method B was followed. White solid; yield 45%; mp 236−242 °C, dec. ^{1}H NMR (500 MHz, DMSO-d_6): δ 7.85 (4H, d, J = 8 Hz), 7.84 (1H, t, J = 8 Hz), 7.64 (2H, d, J = 8 Hz), 7.22 (4H, d, J = 8 Hz), 3.36 (s, 6H); ^{13}C NMR (125 MHz, DMSO-d_6): δ 197.7, 152.8, 143.9, 142.1, 135.8, 131.4, 129.9, 129.2, 128.2, 122.4, 26.7. HRMS (EI+): m/z calcd for $C_{23}H_{18}N_4O_2$ [M − H+]: 381.1352; found, 381.1345.

pK_a Measurement. Measurement of the pK_a values was done by titration of a solution (1×10^{-3} M) of the individual tetrazole examples (**2a**−**e**) in methylcellosolve/water (80% w/w) with a standardized potassium hydroxide solution (0.01 M) using a potentiometric microtitration apparatus. The titration data were analyzed to extract pK_a values and the results of two runs were averaged.

Theoretical Calculations. The conformational analyses of the molecular systems described in this study, including structural and orbital arrangements as well as property calculations, were carried out with the B97-D dispersion-enabled density functional method using an ultrafine grid, in accord with the ansatz proposed by Grimme.[34,35] The B97-D exchange−correlation functional is a special re-parameterization of the original B97 hybrid functional of Becke,[36] which is more neutral to spurious dispersion contamination in the exchange part than the original functional. The Def2-TZVPPD basis set[37] was used for all calculations. Full geometry optimizations were performed both in the gas phase as well as in the solvent and all structures uniquely characterized via second derivatives (Hessian) analysis to determine the number of imaginary frequencies (0 = minima; 1 = transition state) and effects of zero point energy. Effects of solvation were taken into account across a wide range of dielectrics using COSab.[38,39] Relative compound acidity was determined from the computational model reactions: H−CO_2H + X−CO_2H (−) → X−CO_2H + H−CO_2H (−) and H-tetrazole + X-tetrazole (−) → X-tetrazole + H-tetrazole (−). Changes in compound acidity (ΔpK_a values) were analyzed with respect to the dielectric constant of the medium (gas = 0, benzene = 2.27, THF = 7.43, acetone = 20.49, acetonitrile = 36.64, DMSO = 46.83, water = 78.36) and solvent radii from Klamt.[40] See the Supporting Information for further information regarding the choice of these calculation methods for this study. For tetrazole calculations, the 1*H*-isomer was employed. Calculations on the 2*H*-isomer provided a similar result and are included in the Supporting Information.

■ ASSOCIATED CONTENT

Supporting Information

The Supporting Information is available free of charge at https://pubs.acs.org/doi/10.1021/acs.jmedchem.0c02147.

Tetrazole ligands in protein PDB structures; Hammett effect comparison of *p*-X-benzoic acids to 5-(*p*-X-phenyl)-1*H*-tetrazoles; and quantum chemical computational analysis additional details; B97-D/Def2-TZVPPD optimized structures of **1c**, **1c***, **2c**, and **2c***; and B97D/Def2-TZVPPD pK_a trends of 2*H*-tetrazoles **2f**−**h** (PDF)

Discrete structure of 1c-vacuum-b97d_def2tzvppd (PDB)

Discrete structure of 1c*-vacuum-b97d_def2tzvppd (PDB)

Discrete structure of 1c-water-b97d_def2tzvppd (PDB)

Discrete structure of 1c*-water-b97d_def2tzvppd (PDB)

Discrete structure of 2c-vacuum-b97d_def2tzvppd (PDB)

Discrete structure of 2c*-vacuum-b97d_def2tzvppd (PDB)

Discrete structure of 2c-water-b97d_def2tzvppd (PDB)

Discrete structure of 2c*-water-b97d_def2tzvppd (PDB)

■ AUTHOR INFORMATION

Corresponding Author

Jay S. Siegel − *University of California, San Diego, La Jolla, California 92093, United States; School of Pharmaceutical Science and Technology, Tianjin University, Tianjin 300072, P. R. China;* orcid.org/0000-0002-3226-3521; Email: dean_spst@tju.edu.cn

Authors

Brett C. Bookser − *Metabasis Therapeutics, Inc., La Jolla, California 92037, United States; Vertex Pharmaceuticals Inc., San Diego, California 92121, United States;* orcid.org/0000-0002-0822-7029

Quyen-Quyen Do − *University of California, San Diego, La Jolla, California 92093, United States*

Yongsak Sritana-Anant − *University of California, San Diego, La Jolla, California 92093, United States*

Kim K. Baldridge − *University of California, San Diego, La Jolla, California 92093, United States; School of Pharmaceutical Science and Technology, Tianjin University, Tianjin 300072, P. R. China;* orcid.org/0000-0001-7171-3487

Complete contact information is available at: https://pubs.acs.org/10.1021/acs.jmedchem.0c02147

https://dx.doi.org/10.1021/acs.jmedchem.0c02147
J. Med. Chem. 2021, 64, 3197−3203

Funding

This work was supported by the US National Science Foundation and the Swiss National Fonds.

Notes

The authors declare no competing financial interest.

■ ACKNOWLEDGMENTS

J.S.S. and K.K.B. thank the National Basic Research Program of China (2015CB856500) and the Synergetic Innovation Center of Chemical Science and Engineering (Tianjin) for supporting this work.

■ ABBREVIATIONS

FC, flash chromatography; VdW, Van der Waals

■ REFERENCES

(1) Petti, M. A.; Shepodd, T. J.; Barrans, R. E., Jr.; Dougherty, D. A. "Hydrophobic" binding of water-soluble guests by high-symmetry, chiral hosts. An electron-rich receptor site with a general affinity for quaternary ammonium compounds and electron-deficient π systems. *J. Am. Chem. Soc.* **1988**, *110*, 6825−6840.

(2) Cozzi, F.; Cinquini, M.; Annunziata, R.; Dwyer, T.; Siegel, J. S. Polar/π interactions between stacked aryls in 1,8-diarylnaphthalenes. *J. Am. Chem. Soc.* **1992**, *114*, 5729−5733.

(3) Cozzi, F.; Cinquini, M.; Annuziata, R.; Siegel, J. S. Dominance of polar/π over charge-transfer effects in stacked phenyl interactions. *J. Am. Chem. Soc.* **1993**, *115*, 5330−5331.

(4) Meyer, E. A.; Castellano, R. K.; Diederich, F. Interactions with Aromatic Rings in Chemical and Biological Recognition. *Angew. Chem., Int. Ed.* **2003**, *42*, 1210−1250.

(5) Salonen, L. M.; Ellermann, M.; Diederich, F. Aromatic Rings in Chemical and Biological Recognition: Energetics and Structures. *Angew. Chem., Int. Ed.* **2011**, *50*, 4808−4842.

(6) Egli, M.; Sarkhel, S. Lone Pair−Aromatic Interactions: To Stabilize or Not to Stabilize. *Acc. Chem. Res.* **2007**, *40*, 197−205.

(7) Li, S.; Xu, Y.; Shen, Q.; Liu, X.; Lu, J.; Chen, Y.; Lu, T.; Luo, C.; Luo, X.; Zheng, M.; Jiang, H. Non-Covalent Interactions with Aromatic Rings: Current Understanding and Implications for Rational Drug Design. *Curr. Pharm. Des.* **2013**, *19*, 6522−6533.

(8) Kozelka, J. Lone pair-π interactions in biological systems: occurrence, function, and physical origin. *Eur. Biophys. J.* **2017**, *46*, 729−737.

(9) Chen, C.-T.; Siegel, J. S. Through-Space Polar-π Effects on the Acidity and Hydrogen-Bonding Capacity of Carboxylic Acids. *J. Am. Chem. Soc.* **1994**, *116*, 5959−5960.

(10) Duttwyler, S.; Do, Q.-Q.; Linden, A.; Baldridge, K. K.; Siegel, J. S.; Siegel, J. S. Synthesis of 2,6-diarylphenyldimethylsilyl cations: polar-π distribution of cation character. *Angew. Chem., Int. Ed.* **2008**, *47*, 1719−1722.

(11) Padial, J. S.; de Gelder, R.; Fonseca Guerra, C.; Bickelhaupt, F. M.; Mecinović, J.; Mecinović, J. Stabilisation of 2,6-diarylpyridinium cation by through-space polar-π interactions. *Chem.—Eur. J.* **2014**, *20*, 6268−6271.

(12) Simó Padial, J.; Poater, J.; Nguyen, D. T.; Tinnemans, P.; Bickelhaupt, F. M.; Mecinović, J.; Mecinović, J. Stabilization of 2,6-Diarylanilinum Cation by Through-Space Cation-π Interactions. *J. Org. Chem.* **2017**, *82*, 9418−9424.

(13) Bosmans, V.; Poater, J.; Hammink, R.; Tinnemans, P.; Bickelhaupt, F. M.; Mecinović, J.; Mecinović, J. Probing Through-Space Polar-π Interactions in 2,6-Diarylphenols. *J. Org. Chem.* **2019**, *84*, 3632−3637.

(14) Thiolate: Jian, J.; Poater, J.; Hammink, R.; Tinnemans, P.; McKenzie, C. J.; Bickelhaupt, F. M.; Mecinović, J. Through-Space Polar-π Interactions in 2,6-Diarylthiophenols. *ChemPhysChem* **2020**, *21*, 1092−1100.

(15) Lassalas, P.; Gay, B.; Lasfargeas, C.; James, M. J.; Tran, V.; Vijayendran, K. G.; Brunden, K. R.; Kozlowski, M. C.; Thomas, C. J.; Smith, A. B., III; Huryn, D. M.; Ballatore, C. Structure Property Relationships of Carboxylic Acid Isosteres. *J. Med. Chem.* **2016**, *59*, 3183−3203.

(16) For a complete report on the discovery of the first tetrazole containing blockbuster drug Losartan, see Carini, D. J.; Christ, D. D.; Duncia, J. V.; Pierce, M. E. The Discovery and Development of Angiotensin II Antagonists. *Pharm. Biotechnol.* **1998**, *11*, 29−56.

(17) Toney, J. H.; Fitzgerald, P. M. D.; Grover-Sharma, N.; Olson, S. H.; May, W. J.; Sundelof, J. G.; Vanderwall, D. E.; Cleary, K. A.; Grant, S. K.; Wu, J. K.; Kozarich, J. W.; Pompliano, D. L.; Hammond, G. G. Antibiotic sensitization using biphenyl tetrazoles as potent inhibitors of Bacteroides fragilis metallo-β-lactamase. *Chem. Biol.* **1998**, *5*, 185−196. (PDB structure 1A8T)

(18) Narwal, M.; Koivunen, J.; Haikarainen, T.; Obaji, E.; Legala, O. E.; Venkannagari, H.; Joensuu, P.; Pihlajaniemi, T.; Lehtiö, L. Discovery of Tankyrase Inhibiting Flavones with Increased Potency and Isoenzyme Selectivity. *J. Med. Chem.* **2013**, *56*, 7880−7889. (PDB structure 4L34)

(19) Takaya, D.; Niwa, H.; Mikuni, J.; Nakamura, K.; Handa, N.; Tanaka, A.; Yokoyama, S.; Honma, T. Protein ligand interaction analysis against new CaMKK2 inhibitors by use of X-ray crystallography and the fragment molecular orbital (FMO) method. *J. Mol. Graphics Modell.* **2020**, *99*, 107599. (PDB structure 5YVA)

(20) Images of tetrazole ligand molecules in protein binding pockets for this and subsequently cited PDB structures are available in the Supporting Information. Casimiro-Garcia, A.; Heemstra, R. J.; Bigge, C. F.; Chen, J.; Ciske, F. A.; Davis, J. A.; Ellis, T.; Esmaeil, N.; Flynn, D.; Han, S.; Jalaie, M.; Ohren, J. F.; Powell, N. A. Design, synthesis, and evaluation of imidazo[4,5-c]pyridin-4-one derivatives with dual activity at angiotensin II type 1 receptor and peroxisome proliferator-activated receptor-γ. *Bioorg. Med. Chem. Lett.* **2013**, *23*, 767−772. (PDB structure 4HEE)

(21) Zhang, H.; Unal, H.; Desnoyer, R.; Han, G. W.; Patel, N.; Katritch, V.; Karnik, S. S.; Cherezov, V.; Stevens, R. C. Structural Basis for Ligand Recognition and Functional Selectivity at Angiotensin Receptor. *J. Biol. Chem.* **2015**, *290*, 29127−29139. (PDB structure 4ZUD)

(22) Zhang, H.; Han, G. W.; Batyuk, A.; Ishchenko, A.; White, K. L.; Patel, N.; Sadybekov, A.; Zamlynny, B.; Rudd, M. T.; Hollenstein, K.; Tolstikova, A.; White, T. A.; Hunter, M. S.; Weierstall, U.; Liu, W.; Babaoglu, K.; Moore, E. L.; Katz, R. D.; Shipman, J. M.; Garcia-Calvo, M.; Sharma, S.; Sheth, P.; Soisson, S. M.; Stevens, R. C.; Katritch, V.; Cherezov, V. Structural Basis for Selectivity and Diversity in Angiotensin II Receptors. *Nature* **2017**, *544*, 327−332. (PDB structure 5UNG)

(23) Thompson, S. E.; Smithrud, D. B. Carboxylates Stacked over Aromatic Rings Promote Salt Bridge Formation in Water. *J. Am. Chem. Soc.* **2002**, *124*, 442−449.

(24) Du, C. J. F.; Hart, H.; Ng, K. K. D. A one-pot synthesis of m-terphenyls, via a two-aryne sequence. *J. Org. Chem.* **1986**, *51*, 3162−3165.

(25) Bookser, B. C. 2-Benzyloxymethyl-5-(tributylstannyl)tetrazole. A Reagent for the Preparation of 5-Aryl- and 5-Heteroaryl-1*H*-tetrazoles via the Stille Reaction. *Tetrahedron Lett.* **2000**, *41*, 2805−2809.

(26) K_a values for a Hammett series of *p*-X-benzoic acids and 5-(*p*-X-phenyl)-1*H*-tetrazoles: Kaczmarek, J. z.; Smagowski, H.; Grzonka, Z. A correlation of substituent effects with the acidity of aromatic tetrazolic acids. *J. Chem. Soc., Perkin Trans. 2* **1979**, 1670−1674. See Supporting Information for the Hammett plot comparison

(27) Chapman, N. B.; Shorter, J. *Correlation Analysis in Chemistry*; Plenum Press: New York, 1978.

(28) For how this sensitivity affects computational pK_a prediction, see Abramson, R. A.; Baldridge, K. K. Defined-Sector Explicit Solvent in Continuum Cluster Model for Computational Prediction of pKa: Consideration of Secondary Functionality and Higher Degree of Solvation. *J. Chem. Theory Comput.* **2013**, *9*, 1027−1035.

https://dx.doi.org/10.1021/acs.jmedchem.0c02147
J. Med. Chem. 2021, 64, 3197−3203

(29) Rubino, J. T.; Berryhill, W. S. Effects of Solvent Polarity on the Acid Dissociation Constants of Benzoic Acids. *J. Pharm. Sci.* **1986**, *75*, 182−186.
(30) Ghosh, S. K.; Hazra, D. K. Solvent effects on the dissociation of benzoic acid in aqueous mixtures of 2-methoxyethanol and 1,2-dimethoxyethane at 25 °C. *J. Chem. Soc., Perkin Trans. 2* **1989**, 1021−1024.
(31) Boraei, A. A. A. Acidity Constants of Some Tetrazole Compounds in Various Aqueous−Organic Solvent Media. *J. Chem. Eng. Data* **2001**, *46*, 939−943.
(32) Hunter, C. A.; Sanders, J. K. M. The Nature of π-π Interactions. *J. Am. Chem. Soc.* **1990**, *112*, 5525−5534.
(33) Hart, H.; Rajakumar, P. 2′-Substituted meta-terphenyls as building blocks for cyclophanes with intra-annular functionality. *Tetrahedron* **1995**, *51*, 1313−1336.
(34) Grimme, S. Semiempirical GGA-type density functional constructed with a long-range dispersion correction. *J. Comput. Chem.* **2006**, *27*, 1787−1799.
(35) Grimme, S. Semiempirical hybrid density functional with perturbative second-order correlation. *J. Chem. Phys.* **2006**, *124*, 034108−034115.
(36) Becke, A. D. Density-functional thermochemistry. V. Systematic optimization of exchange-correlation functionals. *J. Chem. Phys.* **1997**, *107*, 8554−8560.
(37) Rappoport, D.; Furche, F. Property-optimized Gaussian basis sets for molecular response calculations. *J. Chem. Phys.* **2010**, *133*, 134105.
(38) Klamt, A.; Schüürmann, G. COSMO: a new approach to dielectric screening in solvents with explicit expressions for the screening energy and its gradient. *J. Chem. Soc., Perkin Trans. 2* **1993**, 799−805.
(39) Baldridge, K.; Klamt, A. First principles implementation of solvent effects without outlying charge error. *J. Chem. Phys.* **1997**, *106*, 6622−6633.
(40) Klamt, A.; Jonas, V.; Bürger, T.; Lohrenz, J. C. W. Refinement and Parametrization of COSMO-RS. *J. Phys. Chem. A* **1998**, *102*, 5074−5085.

https://dx.doi.org/10.1021/acs.jmedchem.0c02147
J. Med. Chem. 2021, 64, 3197−3203